

## Fast deposition of carbon and silicon layers

***Citation for published version (APA):***

Beulens, J. J., Buuron, A. J. M., Graaf, de, M. J., Meeusen, G. J., Sanden, van de, M. C. M., Wilbers, A. T. M., & Schram, D. C. (1992). Fast deposition of carbon and silicon layers. *Journal of High Temperature Chemical Processes*, 1(1), 105-127.

***Document status and date:***

Published: 01/01/1992

***Document Version:***

Publisher's PDF, also known as Version of Record (includes final page, issue and volume numbers)

***Please check the document version of this publication:***

- A submitted manuscript is the version of the article upon submission and before peer-review. There can be important differences between the submitted version and the official published version of record. People interested in the research are advised to contact the author for the final version of the publication, or visit the DOI to the publisher's website.
- The final author version and the galley proof are versions of the publication after peer review.
- The final published version features the final layout of the paper including the volume, issue and page numbers.

[Link to publication](#)

***General rights***

Copyright and moral rights for the publications made accessible in the public portal are retained by the authors and/or other copyright owners and it is a condition of accessing publications that users recognise and abide by the legal requirements associated with these rights.

- Users may download and print one copy of any publication from the public portal for the purpose of private study or research.
- You may not further distribute the material or use it for any profit-making activity or commercial gain
- You may freely distribute the URL identifying the publication in the public portal.

If the publication is distributed under the terms of Article 25fa of the Dutch Copyright Act, indicated by the "Taverne" license above, please follow below link for the End User Agreement:

[www.tue.nl/taverne](http://www.tue.nl/taverne)

***Take down policy***

If you believe that this document breaches copyright please contact us at:

[openaccess@tue.nl](mailto:openaccess@tue.nl)

providing details and we will investigate your claim.

## Fast deposition of carbon and silicon Layers

J.J. Beulens, A.J.M. Buuron, M.J. de Graaf, G.J. Meeusen, M.C.M. van de Sanden, A.T.M. Wilbers and D.C. Schram

Department of Physics, Eindhoven University of Technology, P.O. Box 513, 5600 M.B. Eindhoven, The Netherlands

### INTRODUCTION

This paper deals with the plasma physics aspects of plasma deposition in an expanding thermal plasma technique. A summary will be given on previous work on fast a:C-H, graphite, diamond and a-Si:H deposition achieved after a optimization of the plasma process. One of the major themes in plasma deposition is the relation between the composition of monomer fragments, radicals, ions and electrons and the quality of the formed layer. It was generally believed that fast deposition was a negative aspect for quality, the reasoning being that surface migration needed time and that fast deposition tended to overgrow defects. In the history of the present line, deposition rate was the first item. But from the results over the years it became clear, that quality was not necessarily contrary to deposition rate. even crystalline films of good quality were grown with good deposition rates. These facts and particular dependencies as the improvement of deposition quality and rate with increasing ambient pressures in diamond growth, asks for a reassessment of the plasma deposition process. at this point it is unavoidable to make certain simplifications in the picture as there are in many cases not sufficient facts available on composition of the plasma adjacent at the treated surface. Also adsorption - desorption cycles may be important which in turn may influence the radical composition in the plasma adjacent to the surface. Therefore in this paper we will cautiously try to start a discussion, to formulate open questions which we hope will eventually lead to a more concise and effective modeling of the plasma deposition process. We will start the discussion with the summary of findings from more detailed beam experiments on surface physical processes in a plasma environment. From these experiments we will deduce a very simple picture, which, even though it may be oversimplified, can help in explaining results and can guide us to better understand the relation between plasma production, radical and ion fluxes and the deposition rate and quality of the deposited layer.

## MODEL

Since many years it is known that plasma deposition is in fact a balance between etching and deposition in which deposition is dominant. It is also known that in RF etching apparatus for low power and high pressure the balance can switch from etching to deposition. In other words if etch processes act only on poorly bound deposition material it is possible that deposition proceeds with sufficient speed and with less demands to fast surface migration. In this sense it is worthwhile to discuss shortly the outcome of dedicated beam experiments /1-3/. In these experiments the surface is bombarded with an ion beam ( $Ar^+$ ) and a beam of radicals, or molecules which dissociate in radicals at the surface ( $XeF_2$ ). The reactivity at the surface is monitored by observing the desorbing and etched radicals from the surface. In some experiments the energy of the emitted radicals is energy resolved. These experiments give as the first basic fact of plasma processes: there is a synergistic effect of simultaneous ion and radical fluxes e.g. the effect of both fluxes together is larger than the sum of the effect of radicals and that of ions. Even though this synergism is well known and is used to achieve anisotropic etching and selectivity at the same time, it is generally ignored when discussing deposition, and in particular, in discussing the relation between quality and growth rate. In etching it is now generally believed that radicals adsorb and interact with the surface to be etched, and that ions, if sufficiently energy rich, lead to etching in combination with the adsorbed layer and chemically modified top layer of the substrate. This picture explains the anisotropy, as ions are essential, but also the chemical selectivity of the process, as a specific radicalization of the surface is essential. The fact that the process rate may depend on doping /4/ and other qualities of the material to be etched can be explained in such a framework.

One word of caution must be given here regarding two aspects: one is that the intensities of the radical and ion beams are usually lower than those achieved in plasma processes, in particular compared to those reached in the fast deposition apparatus described below. This may be a serious drawback for synergistic processes; nevertheless several experiments with several magnitudes of fluxes have so far led to similar conclusions. A second difference is that the ion energy is usually somewhat higher than in etching processing and considerably higher than in deposition. This will tend to emphasize physical processes in beam experiments, but again it is believed that the above described picture is valid for beam-and plasma-etching experiments. However, no such detailed studies were devoted to study deposition processes as yet because of the evident difficulty to observe the deposited particle compared to the etched particle. Because of lack of these studies,

there is some freedom to put forward a model, which we will use to (over)simplify the picture in the way described below.

In the plasma the monomer gas is dissociated and ionized. Electrons may be attached to form negative ions. So, radicals, which may be vibrationally excited fragments, ions, electrons and negative ions impinge on the surface. In the sheath a potential develops which usually accelerates positive ions, decelerates electrons and prevents negative ions to arrive at the substrate in diffusive situations.

It is difficult to give general estimates of the various fluxes to the substrate. If one takes a RF reactor as an example the net diffusive fluxes to the substrate can be estimated by equating the volume production to the diffusive loss to the substrate /5/. The production is related (due to the existence demands) to the power density /6/. In this way ion fluxes of typically  $10^{19}/m^2.s$  result for power densities of  $10^5-10^6 W/m^3$ , if there is not too much negative ion formation. The radical production and consequently the net flux to the substrate is usually somewhat higher. For many radicals the incoming flux may be orders of magnitude higher than the net flux as the radical density in the plasma may be enhanced by desorption. Still the net flux must obey the production-loss balance. Therefore radical densities may learn more about the adsorption-conversion-desorption cycle than about the contribution of that particular radical to the deposition process. In this respect there is still much controversy and debate in the literature, with as pertinent example the discussion on SiH-, SiH<sub>2</sub> to a: Si-H deposition /7/, /8/.

The above given estimate relates to deposition methods in which the radicals are transported by diffusion. In the situation (to be described below) in which transport is effected by convection flow the situation may be more clear (but not necessarily better). In that case the above described build up of radical densities close to the substrate, due to adsorption-desorption may be less, and radical density measurements are more indicative for the net flow. In view of the above described uncertainties, the still undiscussed role of negative ions and vibrational excitation, we will make rather drastic assumptions, which may clear up the picture, but which may be subject to further discussion /5/.

The first basic and drastic assumption is that at the substrate an adsorbed layer is formed, which is at least several mono layers thick (fig.1). The composition and thickness of this adsorbed layer is determined by several factors /9/. The first is the temperature of the substrate  $T_s$ ; in particular for a: Si-H deposition there has been observed a strong  $T_s$  - dependence of the kind of bonding types /7/8/. Second, the composition depends on the stoichiometric atomic flux composition of the adsorbed layer is determined by only the substrate temperature, the atomic fractions of the radicals and ions incident on the surface and the power flux carried by the

plasma to the surface. This is certainly an oversimplification as several types of radicals or ions may have different sticking coefficients /11/.

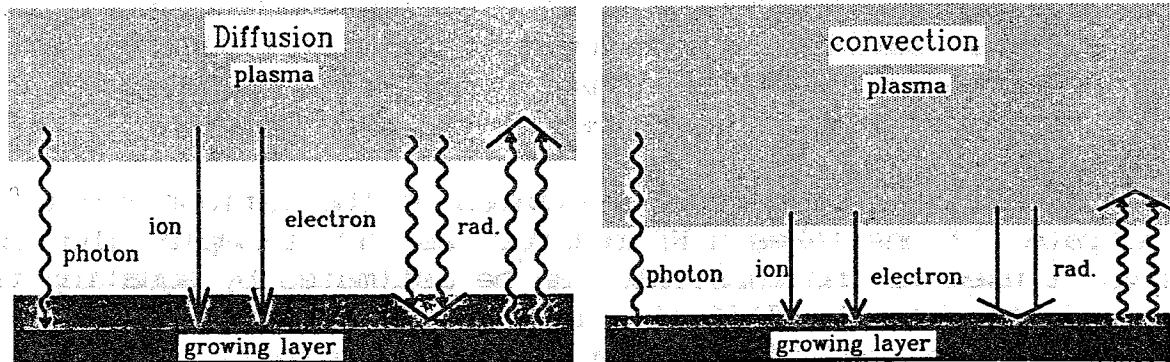


**Fig.1:** Sketch of a plasma deposition model; fig.1a : diffusive transport as e.g. in an RF glow discharge. Typical values for the neutral density ( $n_0$ ), electron- ( $n_e$ ) and ion ( $n_i$ ) densities ( $n_{rad}$ ) are:  $n_e = n_i = 10^{16} \text{ m}^{-3}$ ,  $n_{rad} = 10^{19} \text{ m}^{-3}$  and  $n_0 = 10^{21} \text{ m}^{-3}$ . The sheath voltage is 10-100V, the thickness of the absorbed layer is 0.1-1 mm; fig 1b: convective transport as in expanding thermal arc plasma reactors.  $n_i = n_e = 10^{18} \text{ m}^{-3}$ ,  $n_{rad} = 10^{19} \text{ m}^{-3}$ ,  $n_0 = 10^{21} \text{ m}^{-3}$ . Sheath potential: 1V, Absorbed layer thickness: 1-10 $\mu\text{m}$ . The sheath dimensions are only indicative.

A confirmation that this rather oversimplified picture may have some validity is indicated by the fact that in carbon deposition similar quality material was deposited in two vastly different deposition methods: the classical RF or microwave deposition which is radical rich, and with molecular ions with tens of eV energy and the expanding thermal plasma method which is more atomic ion rich with ion energies in the sub eV range. The only aspect that these two methods had in common is the average energy per deposition event and the temperature of the substrate.

If this picture would be valid, an important consequence would be that high deposition rates would be optimum with ions in the expanding arc deposition method to be described below. The reason is that positive ions can be guided more easily than radicals e.g. by a magnetic field. The magnetic field confines the electrons and therewith the ions. It will appear further that for transport atomic ions are to be preferred to avoid recombination losses. In other words: in this very simple picture high deposition rates would be favored by transport of ions rather than radicals to the substrate. By carefully adjusting the temperature of the substrate and the power flux this could still give sufficient conditions for good quality growth.

At this point it is worthwhile to add one more aspect: the

necessity of an etching gas to promote qualitatively good layers with high rates. For several forms of crystalline growth it has also been shown that high pressure is favorable. This points to an etching of weakly-bonded atoms and recirculation of the etched products through the plasma until a proper bonding site is found or until the particle is lost. In this way this recycling, which will be more effective at higher pressure, may replace partially the need for surface migration to obtain higher quality material. In the following we will first describe the thermal arc expansion deposition method. After a summary of the deposition results, we will return to the picture described above.

### THERMAL ARC EXPANSION PLASMA DEPOSITION

As will be clear without explanation, the primary step for enlarging the deposition rate is enlarging the production rate of electrons, ions and radicals. This is achieved by separating geometrically the production section from the deposition section /12/. High pressure cascaded arcs are most suited for this purpose as then high electron densities are available. Electron kinetics dominate and radiation loss per electron production is less. In other words the energy needed for one ionization event is small; it is typically 2 times the ionization energy /13/. At the start of the program it was generally accepted that at the location of deposition the pressure should be low. (At present, this is not anymore so obvious as will become clear in the next section). This led to the choice of a sub atmospheric arc which expands in a heavily pumped vacuum chamber. The large pressure difference leads to sonic acceleration which minimizes the ion residence time in the arc to  $10^{-4}$ s and therewith minimizes ion and electron loss to the walls of the cascaded arc. In fig. 2 a sketch is given of the cascaded arc particle source /14/, which is described in detail elsewhere /15/. We note here that the cathode side (the high pressure side) is flushed with argon, which is also the carrier gas. Halfway the arc an etching gas as  $H_2$  can be injected; at the end of the arc or in the nozzle the monomer gas is injected in the arc. As stated, the velocity becomes sonic at the end of the arc. Because of the high electron density the heavy particle temperature  $T_h$ , is close to the electron temperature,  $T_e$ , which is in the order of 1 eV. Sonic velocities in argon are close to  $2 \cdot 10^3$  m/s, which is the velocity of the heavy particles inside the plasma jet. Another advantage of the use of thermal plasmas is the full dissociation of etching gas and injected monomers. Since the equilibrium is close to LTE the ionization is transferred to the atom with the lowest ionization potential.

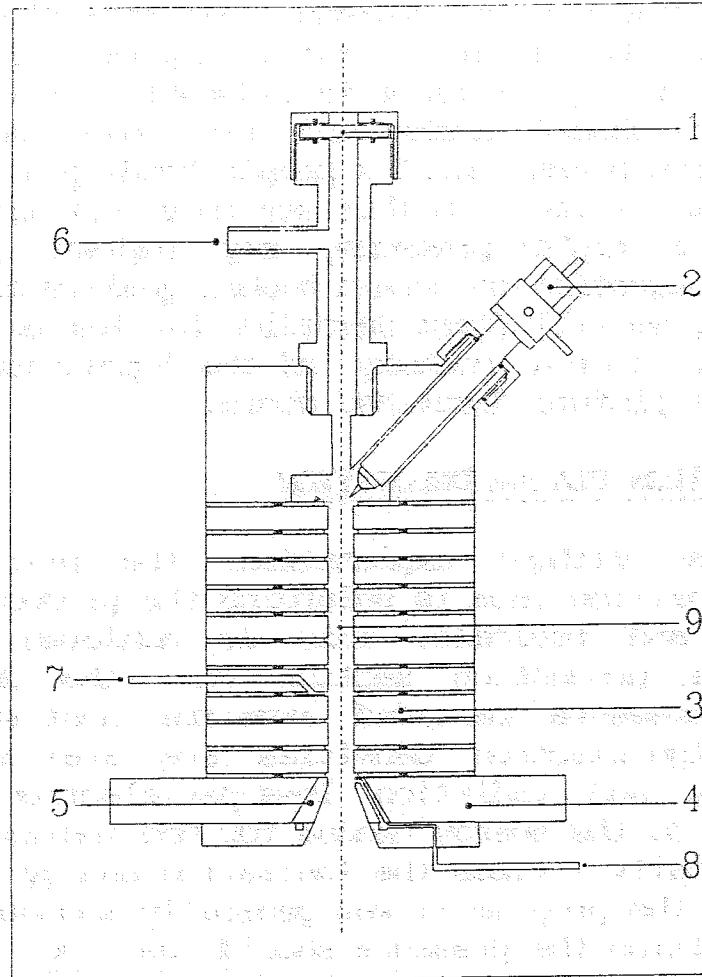


**Fig.2:** Cascaded arc geometry. 1: window, 2: cathode (3x), 3: cascade plates, 4: anode plate, 5: anode insert (nozzle), 6: gas inlet, 7: hydrogen inlet, 8: hydrocarbon inlet 9: Plasma channel. The arc anode is directly mounted on a vacuum system, with a pumping capacity of 0-700l/s.

In fig.3a a comparison is shown between measured and calculated values of the electron density in pure argon. The two dimensional model is based on the conservations laws and is also described elsewhere /16/. the axial dependencies of velocity and pressure are shown in fig.3b and 3c respectively. The ionization degree of the emanating plasma is typically 10%. With 100 scc/s carrier gas this gives an ion fluence of  $2 \cdot 10^{20}$ /s. If  $\text{CH}_4$  is seeded in the carrier gas the ionization is transferred to carbon (ionization potential 11 eV) and to hydrogen, whereas the remaining ions are argon ions.

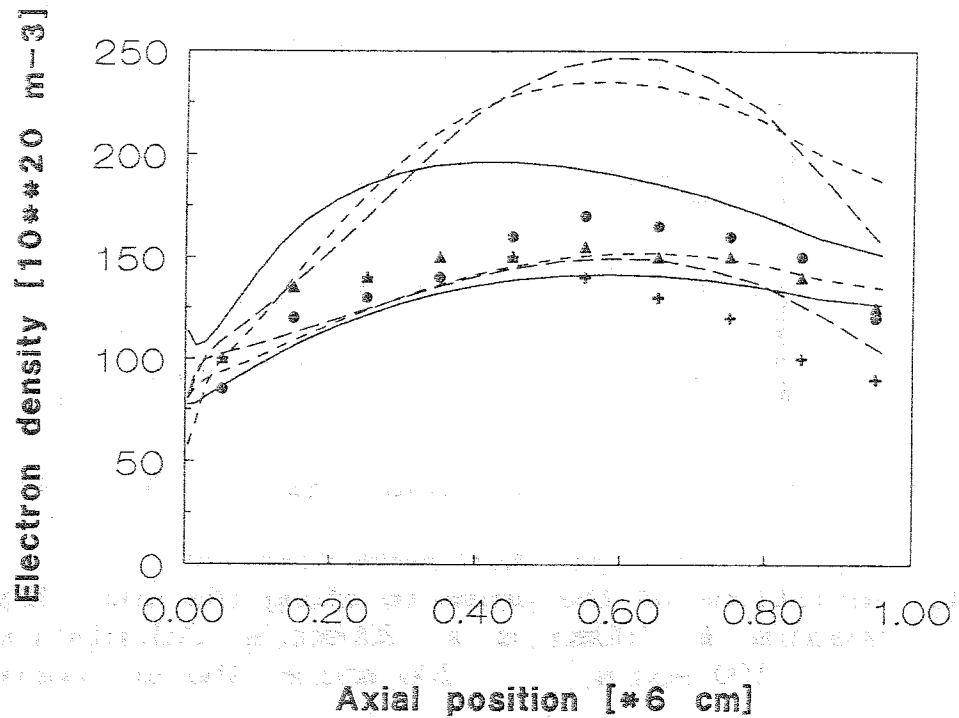


**Fig.3a:** Variation of the electron density along the arc for different argon flow rates. Measurements: +, 50 scc/s,  $\blacktriangle$ , 100 scc/s,  $\bullet$ , 200 scc/s, Calculations: —, 50 scc/s, ---, 100 scc/s, - - -, 200 scc/s. The upper curves are center line electron densities and the lower curves are cross section averaged electron densities.

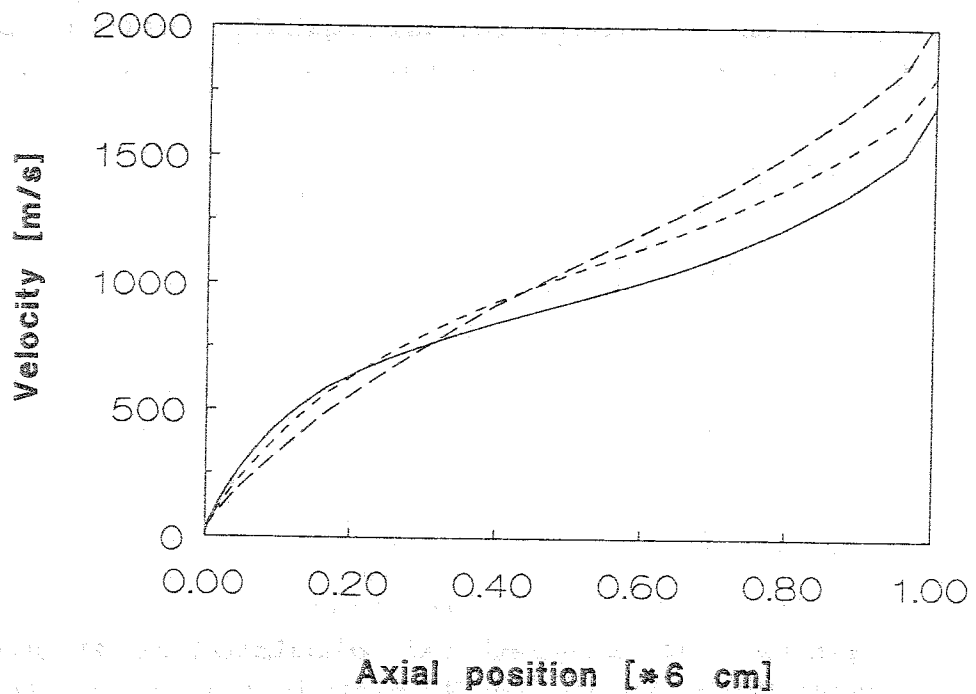


**Fig.3b:** Calculated center line values of the axial plasma velocity along the arc, for different argon flow rates: —, 50 scc/s, ---, 100scc/s, - - -, 200 scc/s. The arc current is 50A



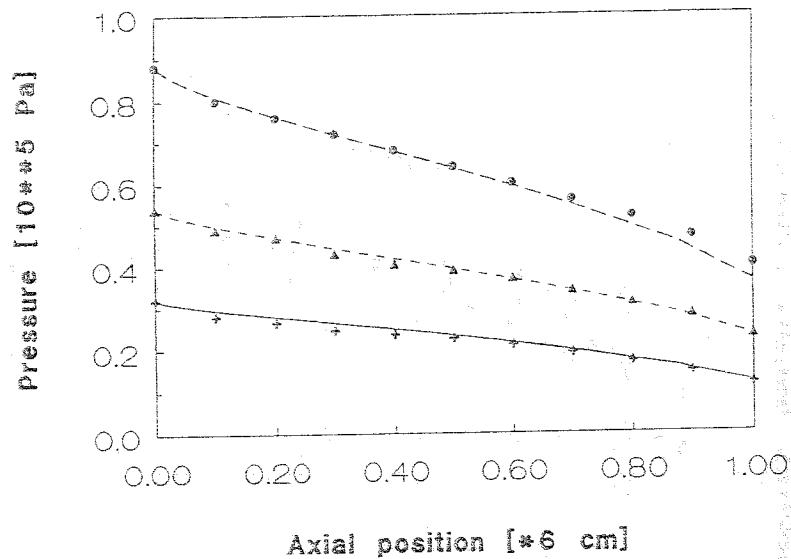


**Fig.3c:** Variations of the pressure along the arc: Experiments: +, 50scc/s, ▲, 100scc/s, ●, 200scc/s, Calculations: —, 50scc/s, ----, 100 scc/s, ---, 200 scc/s. The arc current is 50 A.

An alternative injection location is a ring in the expansion zone. In that case dissociation will be not complete and the monomer structure may be partially retained /14/. Before discussion of deposition results we will first address the physics in the expansion zone.

After emanating from the nozzle, the plasma expands further supersonically; the plasma velocity reaches values of  $4 \cdot 10^3$  m/s. Then, at a distance of about 4 cm from the nozzle a stationary shock occurs after which the plasma expands further subsonically. In fig. 4 the velocity profiles are shown (from ref /15/).

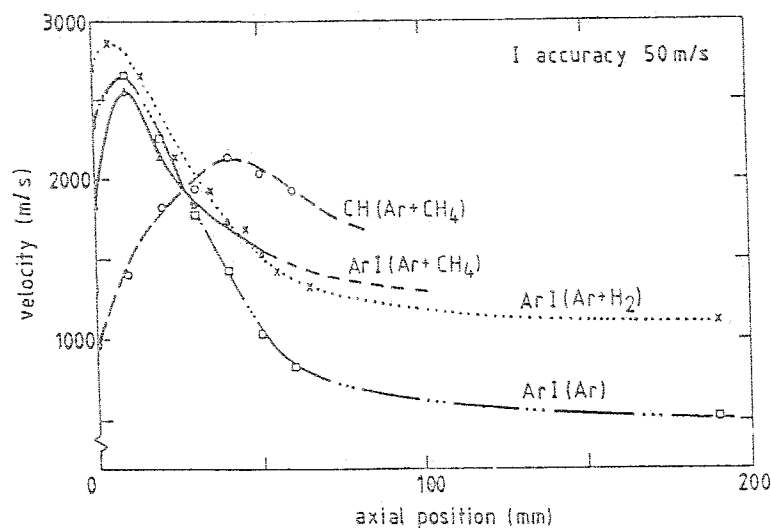


**Fig.4:** Comparison of measured and calculated axial profiles of the plasma velocity in the supersonic expansion followed (after passing the shock wave) by the subsonic relaxation zone. Parameter is the background pressure (20, 100 and 200 Pa). The dashed curves and the points represent the measurements. The full curves correspond to the calculated profiles.

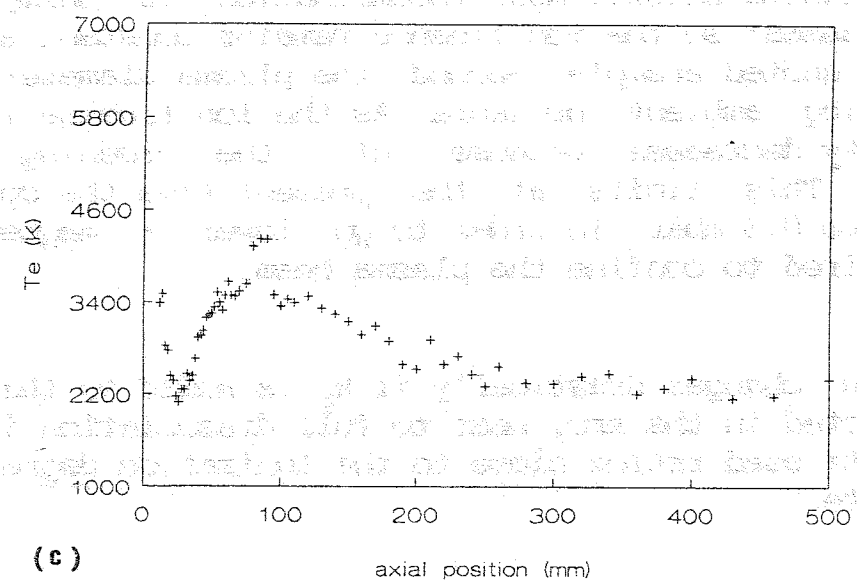
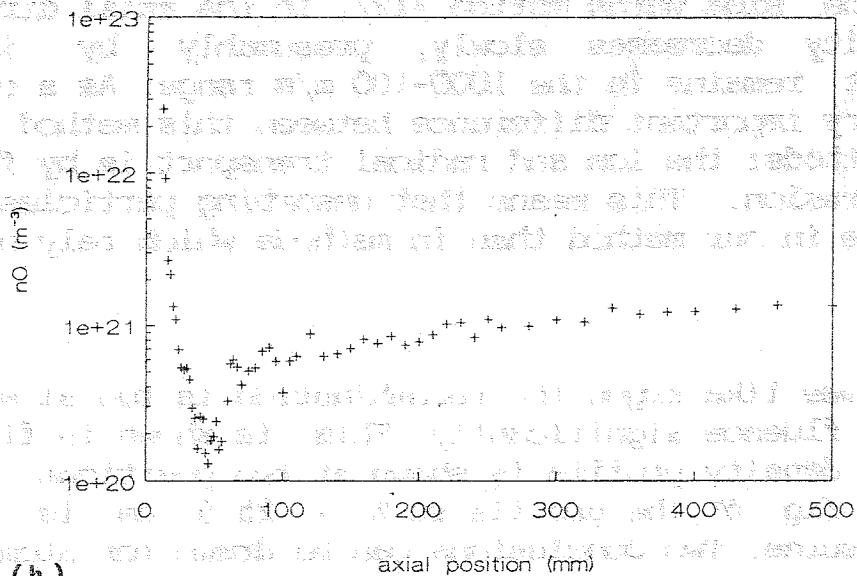
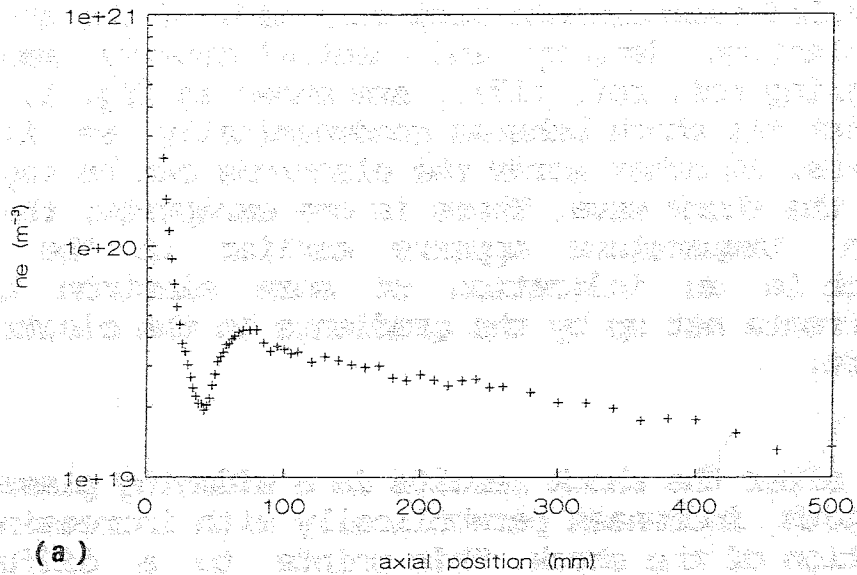


Fig.5: The electron (a) and neutral density (b) and the electron temperature (c) on the axis of the plasma jet for  $I = 45$  A, flow = 3500 ml/min and background pressure  $p = 0.3$  torr.

Recently, detailed measurements have been made of the shock in pure argon. The electron density and neutral density, measured with Thomson scattering (cf. ref. :17/), are shown in fig. 5.

It is clear that the shock behaves gasdynamically as far as the density concerns. In other words the electrons can be regarded as a seed to study the shock wave. There is one exception; the jump in the electron temperature appears earlier in the supersonic expansion which is an indication of some electron heating by convective currents set up by the gradients in the electron density and temperature.

The expansion after the shock results in a widening plasma beam of which the width increases parabolically with increasing distance from the position of the shock. This points to a diffusion like nature of the side wards motion /12/. In the axial direction the plasma velocity decreases slowly, presumably by ion-neutral friction, but remains in the 1000-100 m/s range. As a consequence there is a very important difference between this method and other classical methods: the ion and radical transport is by flow rather than by diffusion. This means that desorbing particles will have less influence in our method than in methods which rely on particle diffusion.

In atomic gases like argon the recombination is too slow to affect the total ion fluence significantly. This is shown in fig. 6<sup>a</sup> /18/ where the ion density profile is shown at two positions,  $Z = 20$  cm,  $Z = 31$  cm. In fig. 6<sup>b</sup> the profile at  $Z = 25.5$  cm is shown for several pressures. Two conclusions can be drawn for atomic gases : First, at pressures below 1 mbar recombination is unimportant in atomic gas plasmas; so the ion fluence remains constant at  $\sim 2 \cdot 10^{20}$  ions/s in the quoted example. Second, the plasma diameter increases with decreasing ambient pressure. As the ion fluence is constant the ion density decreases, because of the widening of the plasma beam. This limits at the present time the operation to pressures above 0.3 mbar. In order to go lower a magnetic field would be required to confine the plasma beam.

The situation changes drastically if  $H_2$  is added to the gas flow. As it is injected in the arc, near to full dissociation is expected and with H/Ar seed ratios close to the ionization degree,  $H^+$  ions should dominate.

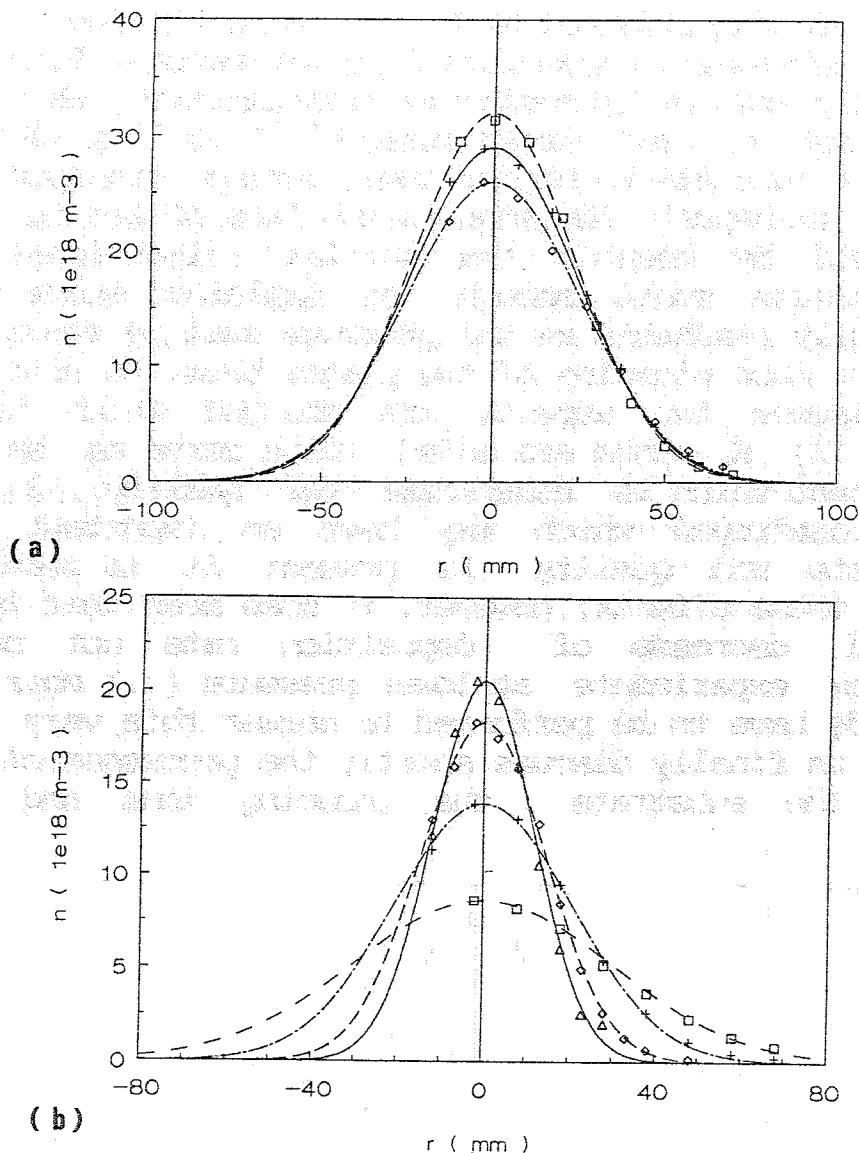


**Fig.6:** a radial ion density profile in an expanding argon plasma at three different axial positions:  $\square$ , 20 cm,  $+$ , 25.5 cm,  $\diamond$ , 31 cm. Background pressure  $p=0.3$  torr, arc current  $I=45$  A, argon flow rate = 3.5l/min.

b Radial ion density profile in an expanding argon plasma for different pressures:  $\square$ , 0.1 torr,  $+$ , 0.3 torr,  $\diamond$ , 0.6 torr,  $\Delta$ , 0.9 torr. Arc current  $I=30$  A, argon flow rate = 3.5l/min.

In fig. 7 again a profile is given, now for a 95% H/Ar-mixture. Note the enormous difference in density scale compared to fig.6. Apparently a very efficient recombination channel is operative. Considering all possible processes there is no other explanation than to assume dissociative recombination because of the large rates. But this requires molecules, and first the conversion of atomic ions ( $H^+$ ,  $Ar^+$ ) to molecular ions should be explained. For the protons, charge transfer between  $H^+$  and  $H_2^v$  -vibrationally excited molecules is the only possibility. If one estimates the partial  $H_2^v >^3$  density to be in the  $10^{18}/m^3$  range, at least qualitatively this route can be explained. Residual  $Ar^+$  ions are

probably lost via formation of  $\text{Ar H}^+$  in a collision with a  $\text{H}_2$  molecule, and subsequent dissociative recombination. Both molecular ions are readily lost by dissociative recombination, which is fast because of high  $n_e$  and large rates  $k^{\text{dr}} \sim 10^{-13}$  à  $10^{-14}$   $\text{m}^3/\text{s}$ . In other words, if ions are to be retained during transport, it is essential to transport the ions in the form of atomic ions. This must be achieved by keeping the partial (vibrational excited) molecular pressure small enough. as explained above this is at present not fully reachable as the pressure must be above 0.3 mbar to avoid too much widening of the plasma beam. So with  $\text{H}_2$  seeded argon arc plasmas two aspects are changed which may affect deposition : 1) H atoms are added, which serve as an effective selective etchant which is beneficial for quality, 2) the ion fraction is destroyed which may have an important impact on deposition rate and quality. At present it is impossible to disentangle these effects; however, it does mean that improvement of quality and decrease of deposition rate not necessarily connected. New experiments at lower pressure ( $< 0.1$  mbar) and with magnetic fields have to be performed to answer this very important question. Let us finally discuss shortly the processes close to the substrate. At the substrate the incoming ions and electrons recombine.

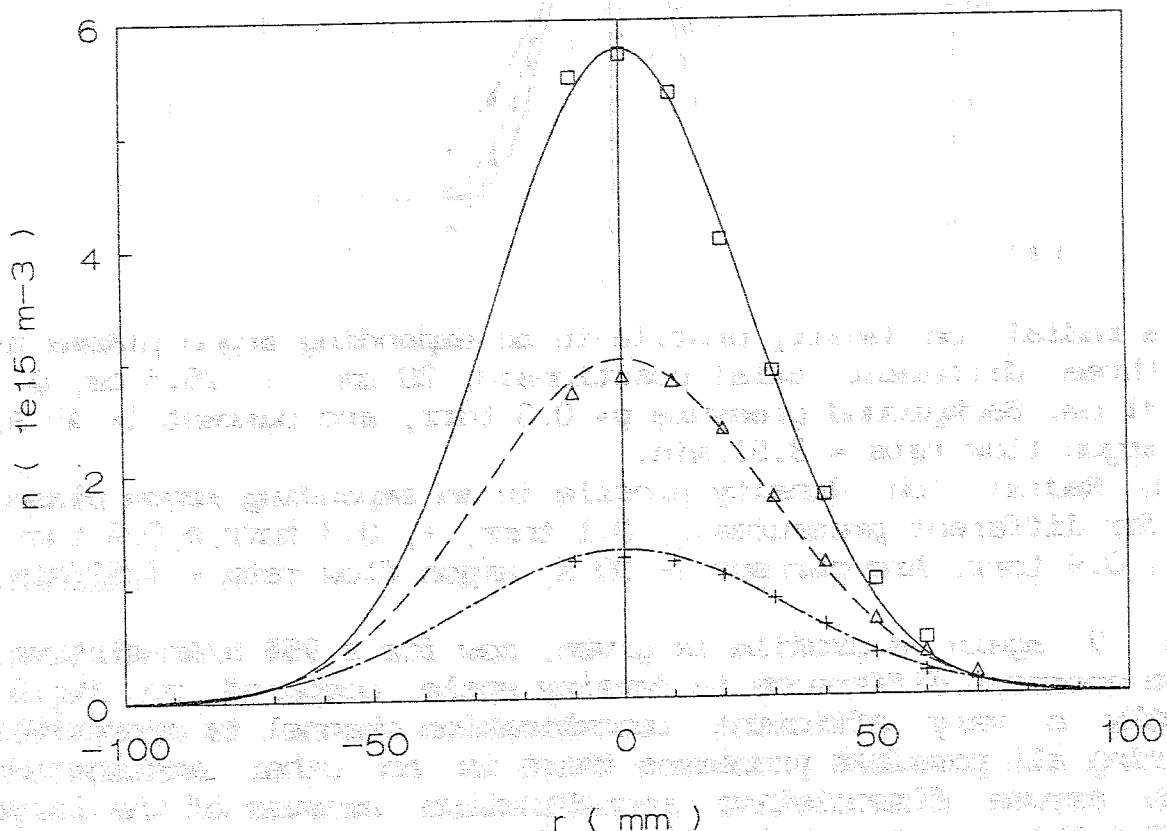


**Fig.7:** radial ion density profile in an expanding argon/hydrogen (5% Ar, 95%  $\text{H}_2$ ) plasma at three different axial positions:  $\square$ , 20 cm + 25.5 cm,  $\diamond$ , 31 cm. Background pressure  $p = 0.3$  torr, arc current  $I = 60$  A, argon flow rate = 3.5 l/min.

In so far this concerns to be deposited particles like  $C^+$ , this recombination could lead to deposition. For  $Ar^+$  and  $H^+$  ions surface recombination will lead to desorbing gas atoms or molecules. Therefore surface recombination contributes to the build up of pressure, just before the substrate. Therefore in the area just before the substrate recirculation vortices could be set up, which will be more prominent at higher pressures. particles at the periphery of the plasma beam will be deflected and contribute to a global recirculation flow in the chamber. Detailed measurements of these flows are still to be done; therefore, only qualitative agreements can be given.

## DEPOSITION RESULTS

### a-C:H films

Over the past years the first and most attention has been paid to amorphous hydrogenated carbon films. These results have extensively been published, so here only a summary suffices /12, 14, 15/.

The amorphous carbon films are produced using only argon (20-400 scc/s) and a hydrocarbon ( $\leq 8$  scc/s) in the setup. The substrate temperature was always between room temperature and  $100^\circ C$  (by water cooling), and the vessel pressure about 1 mbar. The nozzle sample distance was about 70 cm. The deposition rate of this amorphous material proved to be linear with the monomer injection rate up to a maximum where it saturates.

The observed rate is compared in fig. 8 with a calculated rate assuming 100% carbon efficiency. From fig.8 it is clear that a good material efficiency is reached. The differences in saturation rate for  $CH_4$  and  $C_2H_2$  can be explained by the differences needed to fragmentize these molecules and to ionize the resulting atoms ( $\sim 100$  eV/ $C^+$  for  $CH_4$ ,  $\sim 35$  eV/ $C^+$  for  $C_2H_2$ ) which as stated before is reflected in a dependence of the growth rate on the power density. The material structure has been investigated by several techniques. Diffraction (low Energy Electron Diffraction, LEED) and SEM photography do not show any crystalline structures in these amorphous films. Raman spectra show very broad phonon absorption bands which are characteristic for amorphous non crystalline materials. The main film diagnostic tool in our work is ellipsometry /19/. With a He-Ne ellipsometer in situ measurements of the refractive index (n,k) and the film thickness can be performed. In fig.9 the refractive index of the amorphous films is shown as a function of the inverse 'energy' coefficient  $q(W^{-1})$  defined by :

$$Q \equiv \frac{[C_{flow}]}{[Ar_{flow}] [P_{arc}]}$$

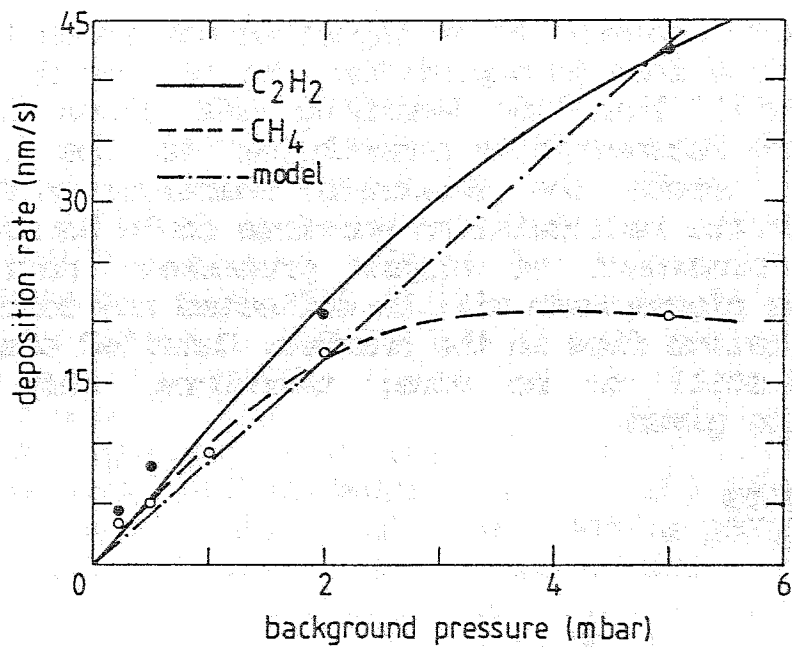


**Fig.8:** The deposition rate as a function of the injected number of carbon atoms for an argon plasma with an admixture of methane or acetylene. The dashed dotted represents calculated values/19/.

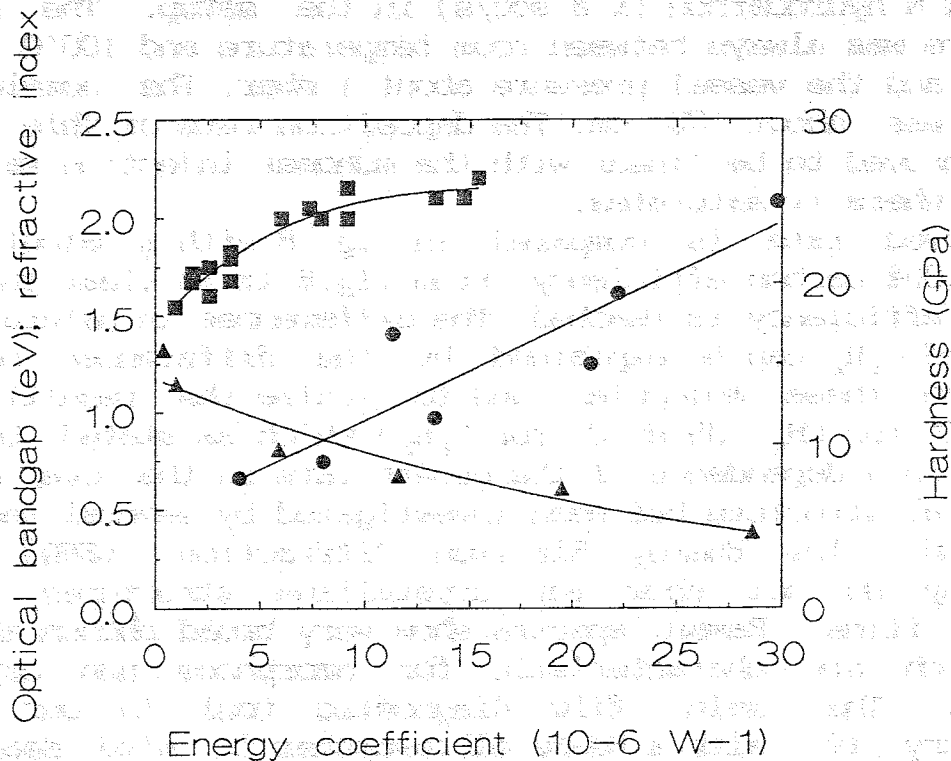


**Fig.9:** Plot of some film parameters vs. the 'energy' factor Q. ■: Refractive index obtained by in situ He-Ne ellipsometry. ▲: The optical band gap (eV) obtained by ex situ spectroscopic ●: Vickers hardness (GPa).

stand  $o/$  stand for the carbon and argon flow rates respectively, and  $/P_{arc}/$  is the arc power in watts. The quantity  $Q^{-1}$  can be seen as the available power, transported by argon, per injected carbon atom. Ex situ these films are studied by spectroscopic ellipsometry /24/. This apparatus is in principle equal to the He-Ne ellipsometer with this respect that here a cascaded arc is used as a light source /20/, with a high spectral intensity in a small angle in a very broad wavelength region, and of course a different detection system. The detection now takes place by a monochromator plus a photo multiplier (250-800nm) or a InSb/HgCdTe sandwich IR detector (2-8.5 $\mu$ m). With this setup the optical band gap, which can be determined from a Tauc plot, and the C-H absorption bands can be measured. The band gap is also plotted vs the factor  $Q$  in fig.9. A typical measurement of the absorption bands is given in fig. 10. In this figure the plasma parameters were such that the factor  $Q$  was small ( $\sim 2 \cdot 10^{-6} W^{-1}$ ), which implies a soft polymer like a:C-H film. The absorption peak at 1450  $cm^{-1}$  may refer to  $sp^2$   $CH^2$  or to  $sp^3$   $CH_2$ . As also a peak is found at 2946  $cm^{-1}$  ( $sp^2$   $CH_2$ ) and not at 2920  $cm^{-1}$  ( $sp^3$   $CH_2$ ) the conclusion is that  $sp^2$   $CH_2$  is one of the prevalent binding forms. The peaks at 1370  $cm^{-1}$  and 2875  $cm^{-1}$  can be attributed to  $sp^3$  CH and  $sp^3$   $CH^3$  respectively /21/.

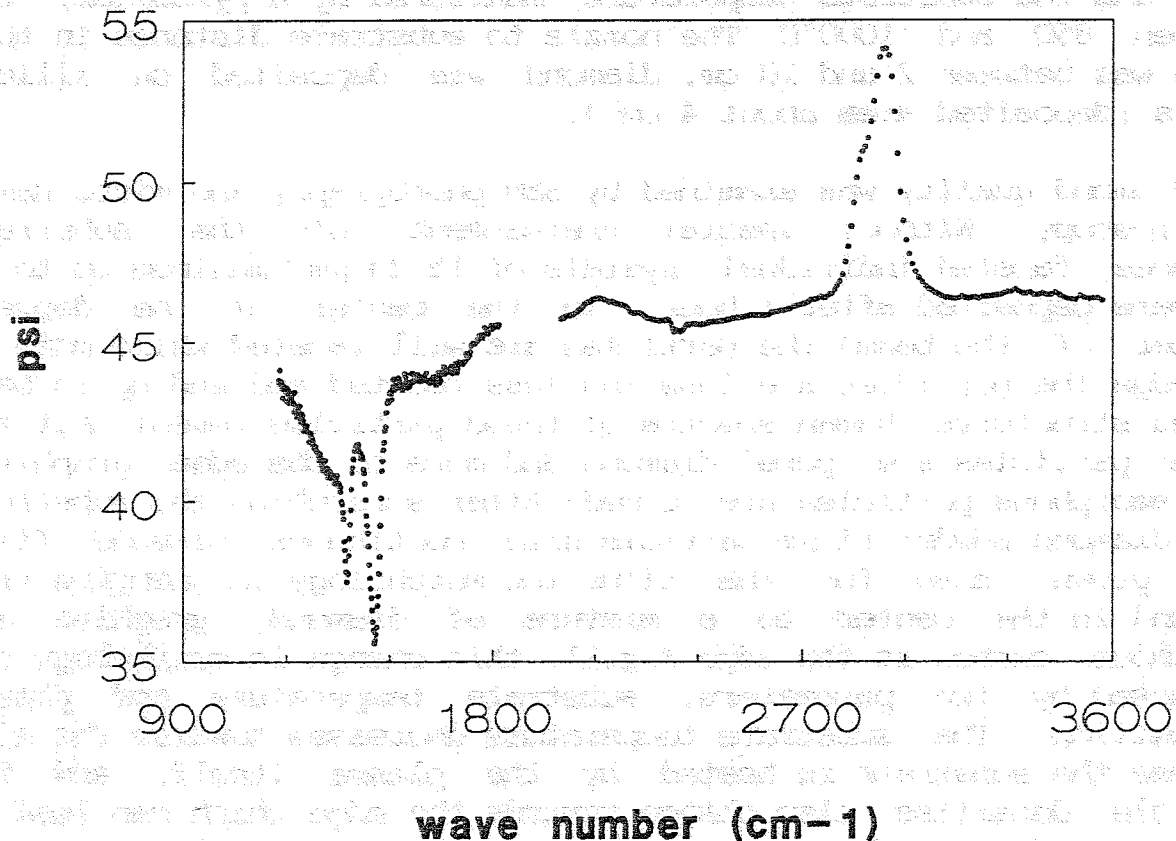


**Fig.10:** Ellipsometric spectrum of a typical polymerlike a-C:H layer. Plotted is the ellipsometric angle  $\psi$  vs. wave number  $\sigma$  ( $cm^{-1}$ ). The parameter  $\psi$  is strongly coupled to the absorption coefficient of the film.



With Rutherford Back scattering the hydrogen content and or depth profile can be measured. A detailed study still has to be done, but some tests reveal that for polymer like films the H contents is about 60% ( $Q < 4 \cdot 10^6 \text{ W}^{-1}$ ) whereas the diamond like coatings ( $Q > 10^5 \text{ W}^{-1}$ ) show a content of 20-30 at%. Also the mechanical property hardness (Vickers) can be plotted vs.  $Q$  in fig. 9 which gives a simple relation between the optical and mechanical properties.

### Diamond

With the same experimental setup it is also possible to grow diamond films /22/. The parameters are quite different from the ones for amorphous films concerning substrate temperature, pressure and hydrogen/carbon ratio. However there is no difference with other deposition techniques like RF plasmas, hot filament or microwave plasmas.

In this work a mixture of 1% methane in hydrogen was used with argon used as carrier gas ( $\text{Ar}:\text{H}_2:\text{CH}_4 = 100:100:1$ ). The pressure in the substrate chamber must be (in our case) larger than about 45 mbar, and the substrate temperature, monitored by a pyrometer, was between 850 and 1000°C. The nozzle to substrate distance in this setup was between 2 and 10 cm. diamond was deposited on silicon wafers (deposited area about 4 cm<sup>2</sup>).

The diamond quality was examined by SEM photography and micro Raman spectroscopy. Without special pretreatment of the substrate surfaces, faceted individual crystals of 15-25  $\mu\text{m}$ , maximum up to 65  $\mu\text{m}$ , were deposited after 1 hour. In the center of the deposit (center of the beam) the particles are well faceted while more to the edge the particles are less and less faceted and end up in ball shaped structures. Raman spectra of these particles reveal that the center particles are 'pure' diamond and more to the edge graphitic and amorphous particles are formed. After scratching the substrate with diamond powder (1  $\mu\text{m}$  particle size) continuous diamond films were grown. also for the films the morphology is changing from diamond in the center to a mixture of diamond, graphite and amorphous carbon at the edge fig.11. this change in morphology can be caused by two parameters: substrate temperature and plasma composition. The substrate temperature decreases towards the edge because the substrate is heated by the plasma itself, and the particle densities also change towards the edge which can lead to different deposited material anyway. As an example also the pressure dependence to the morphology is given in fig. 12. In this figure one can see that when the pressure is decreased graphitic layers are formed. the 1 mbar setting therefore is the starting point for producing graphite layers.

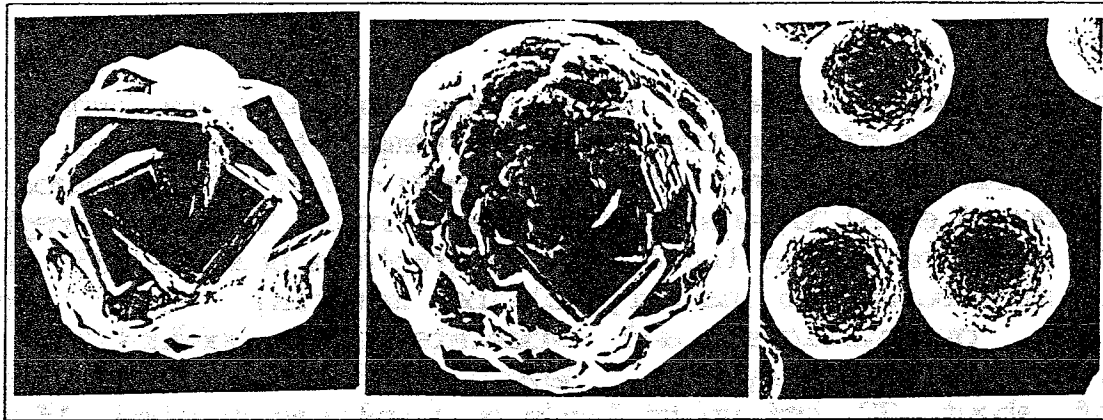


**Fig.11:** SEM micrographs taken at different locations on the same silicon substrate. Near the center of the deposition area high quality crystalline diamond is observed (left). More to the edge of the deposit more and more ball shaped (graphitic, see the right picture) structures are formed.

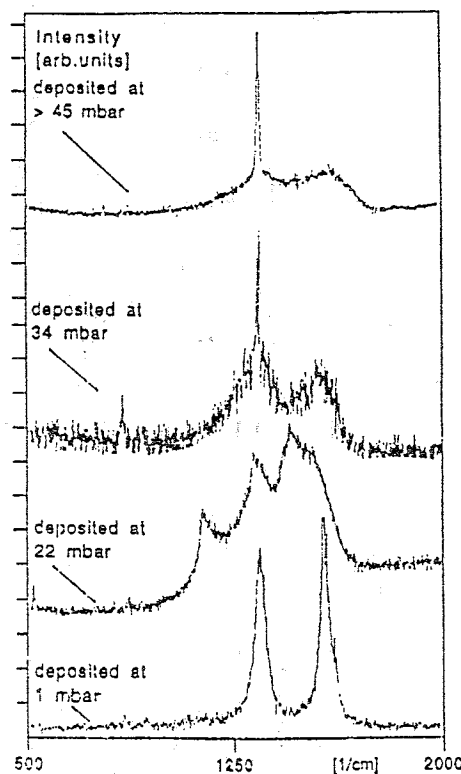


**Fig. 12:** Cascaded arc plasma deposition at different pressure levels. In a series of experiments all other parameters were kept constant. Drastically different materials are deposited. At 1 mbar, only graphite material can be detected by means of Raman spectroscopy. At 22 mbar the nanocrystalline diamond or diamond precursor peaks at  $1150 \text{ cm}^{-1}$  and at  $1470 \text{ cm}^{-1}$  become clearly distinctable. At 34 mbar a narrow diamond peak is already detected and at 45 mbar the common Raman spectrum of a continuous diamond coating (with some impurities) is measured.

## Graphite

To complete the picture for carbon, also graphite was grown/22/. For the deposition of graphite substrate temperatures in the range of 600 to 1400°C are used. In Raman spectra most of the deposited graphite showed equal intensities of the single crystal graphite peak at  $1581\text{ cm}^{-1}$  and the defective graphite peak at  $1355\text{ cm}^{-1}$ . This is attributed to nanocrystalline material with random crystalline orientations and moderate heat conduction. The deposition rates were very high: Several hundreds of nm/s over areas of about  $30\text{ cm}^2$  up to  $1\mu\text{m/s}$  on  $1\text{ cm}^2$  was reached. If more hydrogen was admixed and if the pressure at the deposition location was raised, the material properties were improved considerably, as is demonstrated in the Raman spectra of fig. 13.

In this figure one can see that increasing the hydrogen admixture leads to a decreasing defective graphite peak ( $1355\text{ cm}^{-1}$ ) and an increasing graphite peak ( $1581\text{ cm}^{-1}$ ). The SEM picture of fig. 14 corresponds with the spectrum of fig. 13d. This material could

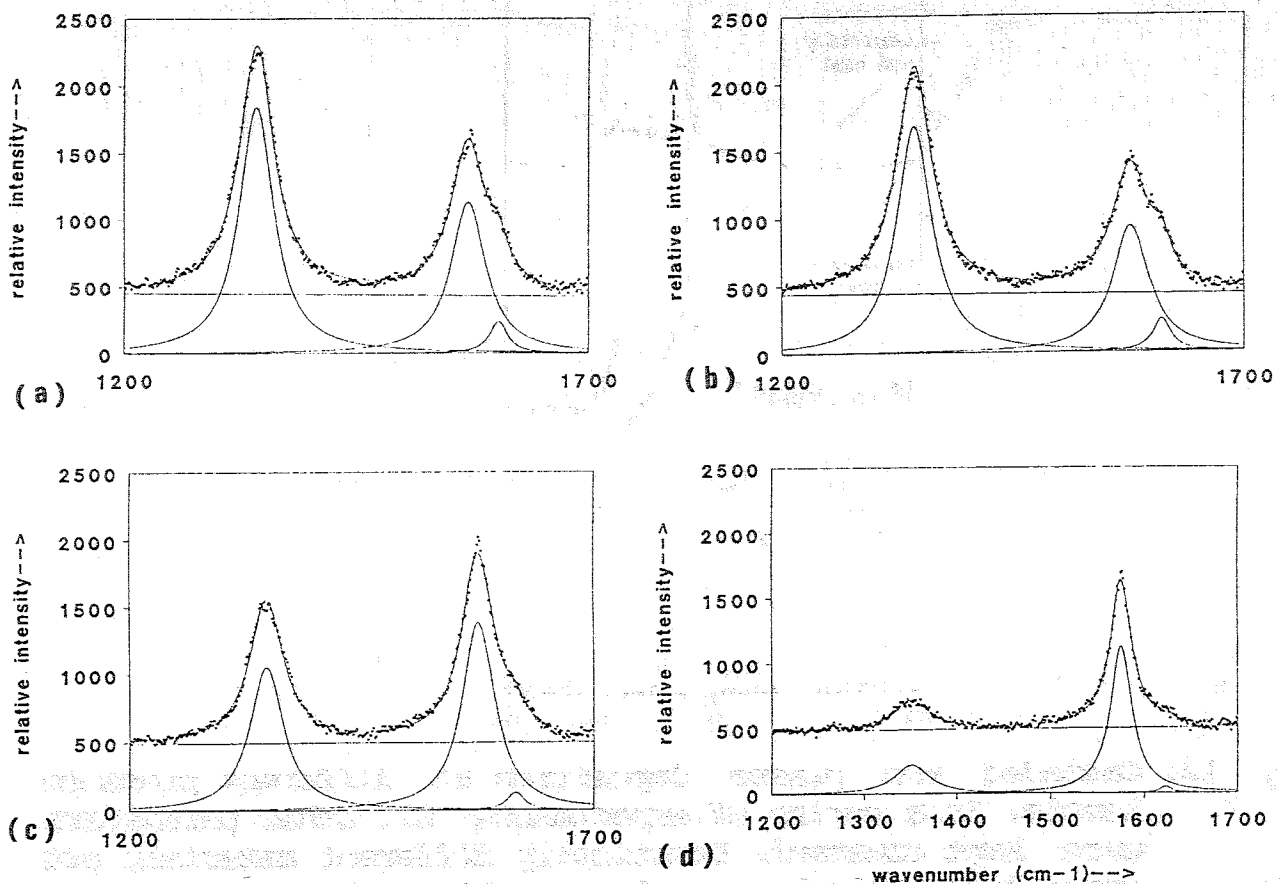


**Fig. 13:** Effect of increasing the hydrogen admixture on the Raman spectra of the deposited graphite (like) layers. from top to bottom (fig.13 a to d) the hydrogen  $\text{H}_2$  admixture was 2.5, 5, 10, and 20 scc/s respectively. The substrate temperature was  $840^\circ\text{C}$ . The growth rate for a to d decreased from 26 to 21 to 12 and to  $13\text{nm/s}$  respectively.

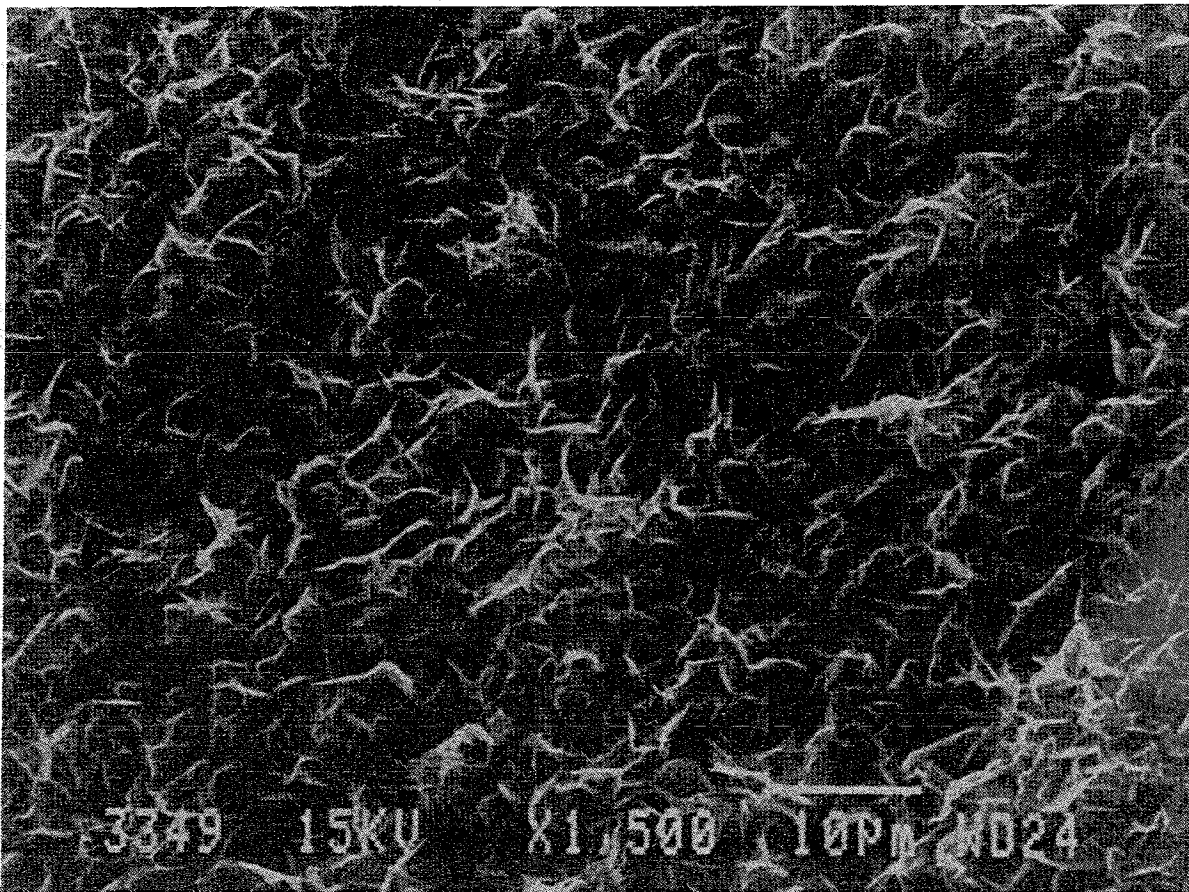


Fig. 14: SEM micro graph of the film with Raman spectrum 13d.

withstand severe heat shocks up to  $3\text{MJ}/\text{m}^2$  in 10 ms. In that case the deposition rate was reduced; it will have values of up to 10-50  $\mu\text{m}/\text{s}$  over areas of  $10\text{ cm}^2$ .

### Silicon deposition

Recently amorphous hydrogenated silicon is produced in a new experimental set up according to the same principle. In this experiment a mixture of 10%  $\text{SiH}_4$ , 90% argon is injected through a ring in the main (argon) plasma flow. This ring is mounted 5 cm downstream the nozzle. The samples are supplied to the vacuum vessel through a load lock system which prevents the vessel of being polluted by other gases than argon, silane or hydrogen. We used four different types of substrates: gold coated stainless steel, gold coated quartz, quartz and silicon substrates. The substrate temperature has been varied between  $100^\circ\text{C}$  and  $300^\circ\text{C}$ . Typical plasma settings were: 5 scc/s  $\text{SiH}_4/\text{Ar}$  mixture 60 scc/s argon. We used spectroscopic infrared ellipsometry to investigate the gold coated samples. Film growth has been monitored by in situ ellipsometry. The other samples have been examined with infrared transmission experiments. We have detected polysilane chains:  $[(\text{SiH}_2)_n]$ ,  $\text{SiH}_2$  and  $\text{SiH}$  bonds depending on the substrate

temperature /24/. With a temperature of roughly  $250^{\circ}\text{C}$  we have detected two types of SiH stretch bonds: one at  $2000\text{ cm}^{-1}$  and one at  $2085\text{ cm}^{-1}$ . Compared to the other samples the strengths of these bonds is relatively low (a factor 10 lower). Also Auger profile measurements have been performed on the gold coated samples. This experiment shows that the gold silicon boundary is smaller than 10 nm. Also a constant concentration of oxygen 2% throughout the layers (600 nm) produced at lower temperatures has been measured. The refractive index of the films is  $1.70 \pm 0.05$  (at  $5\text{ }\mu\text{m}$ ) for the samples produced at temperatures below  $150^{\circ}\text{C}$ . This value lies between those for a-Si:H (3.68, ref. 25) and amorphous  $\text{SiO}_2$  (1.45 ref. 26). The samples produced at higher temperatures have a refractive index of 3.68. The highest deposition rate achieved is approximately 10nm/s, which is about 30 times as high as for conventional RF plasma and CVD methods. In further experiments hydrogen has been added to the main argon flow. Injection halfway the arc proved to give the best results in terms of density of the deposited material and deposition rate.

Further experimentation is needed to search for further improvement of the rate and quality. The first step will be to change the monomer injection from 10%  $\text{SiH}_4/\text{Ar}$ , to full silane. Also the hydrogen onjection and current setting will be tuned such that an optimum is obtained for sufficient H-etching concentration while maintaining a good ionization degree of the plasma.

## DISCUSSION AND SUMMARY

One of the conclusions of the amorphous carbon deposition is that the material properties of the fast grown material in our method is very similar to that grown in other methods. This similarity of results despite the large difference in the energy and kind of fluxes to the substrate and the difference regarding transport by diffusion versus transport by flow points to a validity of the simple "absorbed layer" model described earlier in the paper. Substantiation of this result is very important as its validity gives rise to important consequences. It would indicate that the temperature and the irradiated energy per deposition event would be the determining factors. The way on which the atoms of the to be deposited layers are transported to the substrate would be of less importance. In this framework it would be preferable to use ions as deposition agents as they are more easily transportable; atomic ions are to be preferred as they retain the chemical energy better than the molecular ions in view of dissociative recombination. The results on amorphous silicon with the expansion deposition technique have not yet reached sufficient maturity to draw definite conclusions here. The (known) sensitive dependence on substrate temperature has been confirmed.

The role of admixed hydrogen, which in our method will be fully dissociated, needs further discussion. It has two effects; under certain conditions the material properties improve. It also leads to a decrease of the deposition rate. A simple, and certainly partial, explanation is that H-atoms etch preferable loosely bonded deposited particles. In the absorbed layer picture this would be equivalent to a relative increase of the H-abundance in the composition of the layer, which will shift the equilibrium more to etching, in particular for loosely bonded particles.

However, from experiments also a second drastic consequence of admixing hydrogen has been discovered: it has a devastating effect on the ionization degree of the plasma. It will be unavoidable that this has a negative effect on the ion component of the synergistic deposition process and therewith on the deposition rate. In so far it is the second partial explanation of the decrease of the deposition rate.

At present it is not possible to disentangle the two effects of hydrogen admixture. But it may be that improvement of quality is not necessarily coupled to loss of deposition rate if one could avoid the loss of ionization degree during transport. This forms an important point for future work.

Let us now return to the results on crystalline material. In this case the temperature of the substrate is substantially higher, in the range of 600°C (graphite) to 1000°C (diamond). It is to be expected that the absorbed layer is substantially less developed. As a consequence the relation between the deposition-etching balance and the composition of the plasma adjacent to the surface will be more direct. In particular for the diamond deposition case

the role of an etching agent is essential. In the present case only hydrogen has been tried, but it is known that oxygen works as well. The picture is here that the atomic hydrogen preferentially etches non-diamond-bonded carbon particles. This gives rise to a balance between etching and deposition, in which only a few of the many deposition events lead to successful diamond deposition events. In this picture also the improvement of quality and deposition rate with ambient pressure can be made plausible. At higher pressures the recycling through the plasma will be more prominent and the residence time adjacent to the substrate for H and C containing particles will be prolonged. In fact this forms a very promising factor for plasma deposition, as surface migration can probably be replaced by much faster recycling through the plasma, and also this point certainly deserves more attention.

The etching of graphite in diamond deposition experiments by the overdoses of hydrogen atoms has been confirmed in graphite experiments. In those experiments the admixture of hydrogen is substantially less; in the same order or somewhat larger than the monomer admixture. If it is chosen much larger, than the deposition on graphite substrates shifts to etching. At lower H-admixtures the quality of the graphite improves accompanied by some loss of

deposition rate. As in the diamond case the results are better for higher ambient pressures adjacent to the substrate.

Also in the crystalline case it is not known as yet, which contribution the side effect of ionization loss with increasing H-admixtures has. Experiments are will be done to address this matter in the future.

It is realized that in the present contribution the proposed description model forms only an incomplete basis to address the observed findings. It is insufficient to describe several effects not discussed in this paper as the dependence on deposition or even deposition/etching on the material of the substrate. Using the same plasma conditions and substrate temperature an indication for this effect is shown when diamond was deposited on silicon, etching was observed on graphite substrates, which points to selective deposition in analogy with selective etching. Another example forms the influence of scratching the substrate and the apparent necessity to include an initial growth mechanism in the picture.

Still we hope that this contribution in results and discussion can contribute to further classification of the process and plasma deposition and to finding new ways to improve quality and deposition rate.

#### REFERENCES

- /1/ H.F. Winter, J.W. Coburn, Appl. Phys. Lett. 34, 70 (1979)
- /2/ F.H.M. Sanders, J. Vac. Sci. Technol. B3, 485 (1985)
- /3/ H.A.J. Senhorst, Etching studies in a multiple beam surface experiments. Thesis Eindhoven University of Technology, 1990
- /4/ H.F. Winters, D. Haarer, Phys. rev. B36, 6613, (1987)
- /5/ D.C. Schram, F.J. de Hoog, G.M.W. Kroesen, T. Bisschops, Proc. SASP Conf. (Austria) 1986
- /6/ D.C. Schram, T.H.J. Bisschops, G.M.W. Kroesen, F.J. de Hoog, Plasma Phys. Contr. Fusion, 29, 1353, (1987)  
cf. also :  
T.J. Bisschops, Investigations on a RF plasma related to plasma etching, Ph. thesis, Eindhoven University of Technology The Netherlands, (1987)
- /7/ S. Veprek et al., Plasma Chemistry and Plasma Processing, 10, p. 3, (1989)
- /8/ J. Perrin et al., Conf. Proc. ISPC-9, Pugnochiuso, Italy, 1989
- /9/ G.S. Oehrlein, R. Kalish, Appl. Phys. Lett. 65, 464, 1969
- /10/ D.E Edelson and D.L. Flamm, J. Appl. Phys. 56, 1522, 1984
- /11/ S.M. Gates, Surf. sci, 195, 307, 1988
- /12/ G.M.W. Kroesen, D.C. Schram, M.J.F. van de Sande, Plasma Chem. and Plasma Proc., 10, p. 49, 1990.

- /13/ G.M.W. Kroesen, D.C. Schram, C.J. Timmermans, J.C.M. de Haas, IEEE Trans. on Plasma Science, vol. 18, n° 6, dec. 1990.
- /14/ J.J. Beulens, G.M.W. Kroesen, D.C. Schram, C.J. Timmermans, P.C.N. Crouzen, H. Vasmel, H.J.A. Schuurmans, C.B. Beyer, J. Werner, J. of Appl. Polymer Sc, 46, Boston, Massachusetts, 1990.
- /15/ D.C. Schram, G.M.W. Kroesen, J. de Haas, Int. Workshop "High Temperature Dust-Laden Jets...", Novosibirsk, USSR, sept., 1988.
- /16/ J.J. Beulens, D. Milojevic, D.C. Schram, P.M. Vallinga, Submitted for publ. in Phys. of Fluids B: Plasma Phys., 1991.
- /17/ M.C.M. van de Sanden, G.J. Janssen, D.C. Schram, and B van der Sijde, to be published.
- /18/ M.J. de graaf, R.P. Dahiya, J.L. Jauberteau, F.J. de Hoog, M.J.F. van de Sande and D.C. Schram, Colloque de Physique, Colloque C5, suppl. au n° 18., Tome 51, 1990
- /19/ G.M.W. Kroesen, Ph. D. Thesis, Eindhoven University of Technology, The Netherlands, 1988.
- /20/ A.T.M. Wibers, Ph. D. Thesis, Eindhoven University of Technology, The Netherlands, 1991.
- /21/ B. Dischler, R.E. Sah, and P. Koidl, conf. Proc. ISPC-7, Eindhoven, The Netherlands, 45, 1985.
- /22/ P.K. Bachmann, H. Lydtin, D.U. Wiechert, J.J. Beulens, G.M.W. Kroesen, and D.C. Schram. Proc. 3<sup>rd</sup> Int. Conf. on Surface Modification Techn., p. 69, sept. 1989, Neuchatel Switzerland.
- /23/ A.J.M. Buuron, J.J. Beulens, M.J.F. van de Sande, and D.C. Schram, in press in Fusion Technology, 1991.
- /24/ A.T.M. Wilbers, G.J. Meeusen, M. Haverlag, G.M.W. Kroesen, D.C. Schram, H. Kersten, accepted for publ. in Thin Solid Films, 1991.
- /25/ J.D. Joannopoulos, and G. Lucovski, "The physics of hydrogenated amorphous silicon...", Springer Verlag, Berlin, Heidelberg, New-York, Tokyo, 1984.
- /26/ E.D. Palik, "Handbook of optical constants of solids, Academic Press, inc., 1985.